の確立に向けたこれらの取り組みに貢献してきたわれわれの研究成果の一部と，それらの研究結果から帰納的に導き出された慢性影響評価研究の重要性について論ずる．

2. ナノマテリアルのリスク評価法の確立における課題

一般的に，化学物質の健康影響評価（リスクアセスメント）の基本的なフレームは，有害性評価と曝露評価，及び各々の評価内容を比較・統合化する過程のリスク判定のステップから成り立っている．この基本的なフレーム自体は，ナノマテリアルの健康影響評価に適用できるものであると考えられる．[1-5] しかし，ナノマテリアルに特徴的な新たな物理化学的性質，特にサイズが生体内高分子と近いことや，高い表面活性のために凝集し易い性質を考慮すると，よりサイズの大きい通常のバルク化合物や完全に溶解した単一分子化合物とは，生体内挙動が異なることが予想され，同じ化学組成の化合物であってもその毒性発現部位や発現様式は異なることが予想される．つまり，体内動態［吸収 absorption，分布 distribution，代謝 metabolism，排泄 excretion (ADME)］情報は，一般の化学物質より重要な意味を持つと考えられる．

そこで，生体内での挙動を把握するためには，生体試料中で検出，同定・定量できる方法を確立しなくてはならない．一般にナノマテリアルの開発段階において，その性質を把握するための物理化学的測定法も同時に開発されているはずであるが，それらの手法は生体試料中に存在するナノマテリアルにそのまま適用できないことも多い．さらに，機器分析法による生体試料中での検出や定量が可能になったとしても，生体内で実際にナノの状態で存在しているのか，あるいは再凝集などはしていないかなど，標的組織における最終的な生体内反応に影響を及ぼすと考えられる実際のナノマテリアルの存在状態を把握するためには，最終的には，組織標本の電子顕微鏡などによる確認が必要となる．

一方，体内動態に影響を与える因子として，投与法を検討する必要もある．単独では凝集し易いナノマテリアルをそのまま曝露するということは，物理的に巨大となった粒子は体への吸収性が低く，ナノマテリアル自体の体内動態や懸念される有害性を検出することが困難になると考えられるためである．そのために曝露実験時におけるナノマテリアルの分散手法の開発が必要となる．職業曝露などの比較的大量のナノマテリアル曝露の安全性を評価するという観点からは，凝集したままの曝露にも意義があるかもしれないが，製品中への混入や環境中への排出を経由した，分散された曝露も想定されることは考慮すべきであると考えられる．

Figure 1 は，凝集したナノマテリアルが，生体に取り込まれた場合に想定される体内動態を模式図化したものである．ナノマテリアルの使用用途にも依存するが，製品中のナノマテリアルはポリマー等の他の高分子化合物等と混合された状態，あるいはナノマテリアルだけが単独で製品から解離していく状態を考慮しても，この凝集性のために，大きな粒子として曝露する可能性が高いものと想定される．急性的には，このサイズの大きくなった物質は生体に取り込まれることはほとんどなく，局所的な刺激を起こすような変化を除いては，生体内で有害性が惹起される可能性は低いものと考えられる．しかし，仮に凝集したナノマテリアルが長期間に渡って，吸収部位である肺胞や消化管，損傷皮膚などの局所に滞留したり，慢性的に曝露したりするケースを想定すると，時間経過とともに小さくなった凝集体の粒子を除去するために，マクロファージなどの食細胞による取り込みや，表面活性の高いナノマテリアル分子と生体成分との結合作用による侵食作用により，生体に少しずつ取り込まれることが想定される．もしも生体内に取り込まれたナノマテリアルと生体内成分との結合性が高い場合には，容易に生体外に排出されることはなく，特定の組織等へ蓄積し易くなり，慢性影響の可能性を検討する必要が出てくると想定できる．

3. 国立医薬品食品衛生研究所における取り組みの成果の概要

以上のナノマテリアル固有の検討課題を考慮して，われわれは 2005 年より厚生労働科学研究の化学物質リスク研究事業の枠組みの中で，ナノマテリアルの健康影響評価手法の開発に係わる研究を推し進めてきたところである．われわれは，これらの検討課題を解決するために，Fig. 2 に示すように 4 つの項目を中心に研究を行ってきた．これらの項目の中で，*in vivo* 研究については，比較的研究初期の段階から中心的に取り組んできた．その中で，繊維

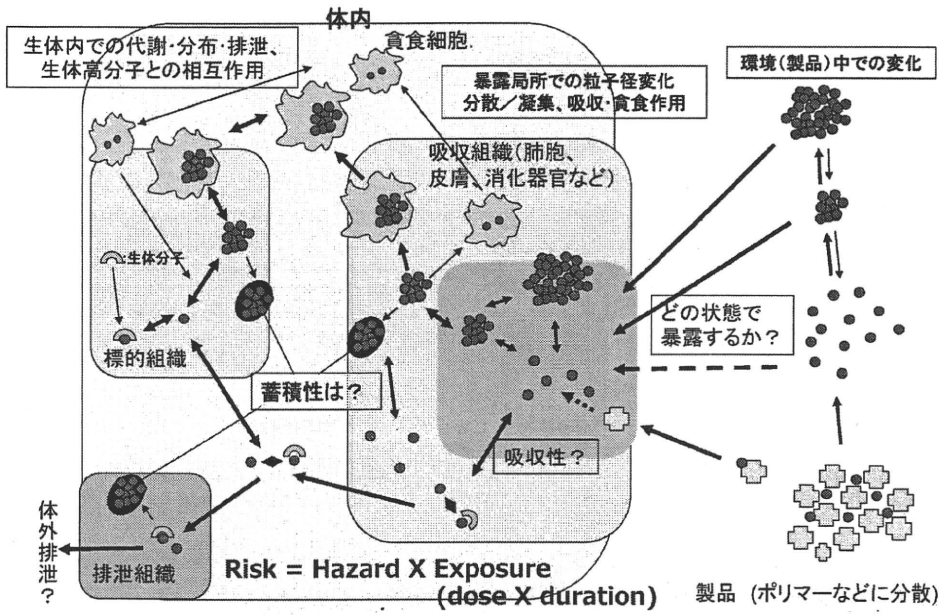

Fig. 1. The Estimated ADME Schema of Nanomaterials

***in vivo*試験法研究**

MWCNTのP53ヘテロ欠失マウスへのi.p.投与による中皮腫誘発性を確認
バイオマーカとしてマウスのメソセリン抗体の作成
一方、C60の腹腔内投与による慢性的影響として腎臓への影響を示唆
TiO_2と C60の気管内投与による発がんプロモーション作用の示唆

吸入試験法研究

MWCNTのミスト暴露システムを開発
気管内投与時の分散性依存の発現様式差異を確認
リポソーム分散C60による気管内投与法を開発。

暴露測定法／動態解析研究

生体試料でのC60の定量的検出法との確立
静注後のC60の組織からの経時的消失検討
気管内投与後のMWCNTの肺及び肝臓での検出

***in vitro*試験法研究**

細胞培養系でのリポソーム等を用いた分散法の確立
→C60やTiO_2の遺伝毒性、細胞透過性、
神経系の細胞機能への影響、などへの適用

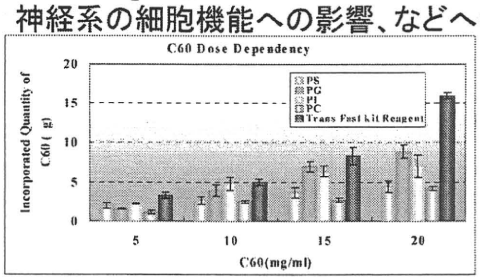

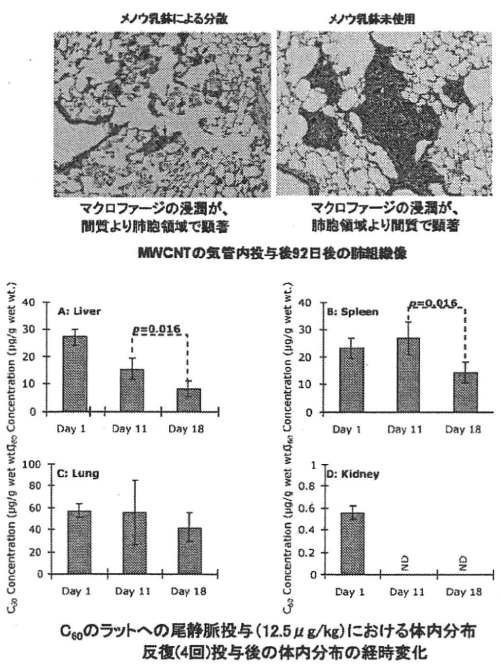

C_{60}のラットへの尾静脈投与(12.5 μ g/kg)における体内分布
反復(4回)投与後の体内分布の経時変化

Fig. 2. The Overall Results of NIHS Projects for Nanomaterial Safety

長の長いタイプの多層型カーボンナノチューブ（MWCNT）が，中皮腫を誘発する可能性を持つことを確認した.[6] 上記の体内動態の重要性を考慮した概念からは，吸収性や体内分布について検証したのちに，慢性影響の可能性を検討することが論理的であるが，研究開始当時から，大量生産可能であった，酸化チタン（TiO_2）やフラーレン（C60），MWCNTについては，*in vivo* の慢性影響を先行して検討しておくべきであると判断した．特にその形状がアスベストに似ていたMWCNTについては，吸入曝露による有害影響が懸念されたが，MWCNTについての吸入曝露法が確立していない段階では，アスベストでも検証に使用されていた腹腔内投与による中皮腫誘発試験を行うこととした．

われわれの最初の実験は，アスベストで中皮腫の誘発時期が早くなることが知られているp53ヘテロノックアウトマウスへの腹腔内へ3 mg/mouseという高用量を投与することによって確認されたものであり，動物種の特異性や投与量の多さについて異論も指摘された．しかしその後の研究で，野生型の動物種であるF344ラットに対しても，同じMWCNTが中皮腫の誘発作用を持つことが確認された[7]ほか，投与量を1000分の1にまで少なくした実験においても中皮腫の起きることが示されている（投稿中）．

酸化チタンについては，雌ラットへの吸入曝露により発がん性のあることが示されているが，ナノサイズ化による発がん性の検証のために，気管内投与による肺がんのプロモーション作用の検討を行った．その結果，酸化チタンは，肺腺腫や乳腺腫に対してプロモーション作用を示し，その作用は，マクロファージから放出される炎症性因子であるMIP1αを介したものであることが示唆された.[8] 現在C60やMWCNTを用いたプロモーション作用の検討が進行中である．

一方，曝露手法の開発においては，ミスト法や粉体法によるMWCNTの吸入曝露システムの開発研究を進めているが，より簡易な手法として気管内投与のための適切な分散法の検討を行った．その結果，分散法の違いが肺の有害性発現様式に違いを引き起こすことを確認した.[9]

体内動態解析のために，生体試料中のC60やTiO_2の分析手法の開発や改良を行い，経口投与や気管内投与による体内吸収性について検討を行っている．現在のところ投与部位である消化管や肺以外で有意な検出量を確認できておらず，感度の向上に向けた研究を進めている．しかし，体内への吸収を前提にした解析として，C60の静脈内投与による解析を行ったところ，肝臓や脾臓，肺などへの分布を確認したが，腎臓への分布は極めて低いことが示された（投稿中）．その他，遺伝毒性や標的臓器などの毒性をスクリーニングするための *in vitro* 試験における培地等への分散法も検討対象としており，リポソームを用いたC60の分散法を確立した．

4. 慢性影響研究の重要性

ナノマテリアルの生体影響に関する情報はここ数年の活発な研究状況を反映して多くなりつつあるが，慢性影響に関する報告は依然その数が少ない状況である．一般の化学物質の有害性評価の常套手段として，変異原性試験や短期試験から情報を収集していくことは，必要なステップであり，OECDにおけるナノマテリアル作業グループの活動におけるスポンサーシッププログラムにおいても，加盟各国からの毒性試験情報として，短期試験を中心に収集されてきている．われわれの研究グループにおいても，これらの枠組みに対して，短期的な試験情報を中心に提供し始めている段階である．しかしMWCNTに関しては，研究初期から，短期毒性より長期毒性の方が懸念の強いことが，物性等の情報から推測されたところでもあり，その推定に基づいて，腹腔内投与の研究を最初にスタートさせた．腹腔内投与は，リスク評価の観点からは，曝露経路（吸入曝露）に伴う定量的な評価に問題のあるところであるが，最近の注目すべき研究として，分散剤で分散させたMWCNT（最高80 μgまで）をマウスに吸引させた研究や，MWCNT: 30 mg/m^{3}をマウスに単回吸入曝露した研究において，曝露後7–8週間目にMWCNTが胸膜に到達していたことが報告されている.[10,11] これらの研究結果は高用量の曝露による短期間の結果ではあるが，呼吸器を経由した曝露においてもMWCNTは胸膜（中皮）まで到達することを示唆しており，われわれの腹腔内投与による結果と合わせると，リスク評価の上でも重要な知見であると考えられる．

これらの腹腔内投与による中皮腫誘発能は，繊維状粒子による催腫瘍性のみを検出する系であり，短

いタイプやその他様々な形状の MWCNT における慢性毒性は別途検証する必要性がある．実際，われわれの行った腹腔内投与試験では，小さいサイズのナノチューブ繊維を含んだ細胞が腹膜の病変部のみならず，肝類洞内，又は肝葉間や腸間膜リンパ節の中にも認められ，体内に再分布することが示唆された（Fig. 3）.[6] さらに，SWCNT をマウスへ咽頭吸引させた実験では，一過性の急性症状の後に，炎症性細胞浸潤を伴わない間質の繊維化が認められている.[12] また，ApoE ノックアウトマウスを用いた実験では，タンパクカルボニル化活性の変化を伴うミトコンドリア DNA 障害と，アテローム性動脈硬化症の進行を増強することが示された.[13] MWCNT に関しても，マウスに MWCNT（200–400 μg）を気管内滴下した実験では，一過性の肺の炎症反応に加え，投与量に依存した血小板の活性化と凝固作用の活性化の促進が示唆されている.[14] また，MWCNT や SWCNT の気管内投与や経鼻投与により，アレルギー反応の増強反応が報告されている.[15–17] これらの結果が，カーボンナノチューブが直接体内循環に侵入した結果であるか，免疫細胞との接触を介した反応であるかを区別することは難しいが，曝露局所に留まらない全身作用の可能性を示している．われわれの酸化チタンの気管内投与による発がんプロモーション作用が，炎症因子により介在されたことは，これらの知見と同様の作用様式を示すものととらえることもできる．

以上の知見は，短期の試験だけでは検証することは困難であり，ナノマテリアルの有害性を確認するためには，長期の体内動態予測や慢性影響に関する研究が，重要なステップであることを示している．Figure 4 にスクリーニング試験や確定試験を開発するための手順についてまとめた．通常の化学物質については，その長い歴史の中で明らかとなった有害性に対して，それぞれの毒性発現様式に応じてスクリーニング試験が開発され，現在まで運用されてきている．特に変異原性試験は発がん性を予測する試験としての重要な役割を担っている．しかし，現時点ではナノマテリアルによる有害性影響が，これまでの研究経験の中で明らかとなった影響だけに留まるのかについては，まだ誰も判定できない状況である．これまでの一般化学物質に対応する有害性とスクリーニング試験を活用して進めていくと同時に，未知の影響を見極める最初のステップとして，少な

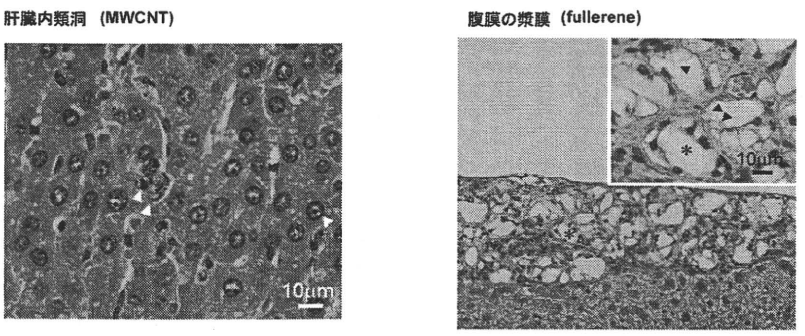

A. Takagi et al., J. Toxicol. Scie., **33**,105-116. (2008)

SWCNTやMWCNTによる全身性影響の示唆

- アテローム性動脈硬化症の進行の増強の可能性（ApoE$^{-/-}$マウス）
  Z. Li *et al.*, *Environmental health perspectives*. **115**, 377-382 (2007)
- 血小板の活性化と凝固作用の活性化（MWCNT気管内滴下）
  A. Nemmar *et al.*, *J. Thrombosis, Haemostasis* **5:** 1217-1226 (2007)
- アレルギー反応の増強（MWCNT・SWCNT、気管内・経鼻投与）
  E.J. Park *et al.*, *Toxicology*. **259**, 113-21 (2009)
  U.C. Nygaard *et al.*, *Toxicol Sci*. **109**, 113-23 (2009)
  K. Inoue *et al.*, *Toxicol Appl Pharmacol*. **237**, 306-16 (2009)

Fig. 3. The Suggestive Evidences for Systemic Toxicites by Nanomaterials

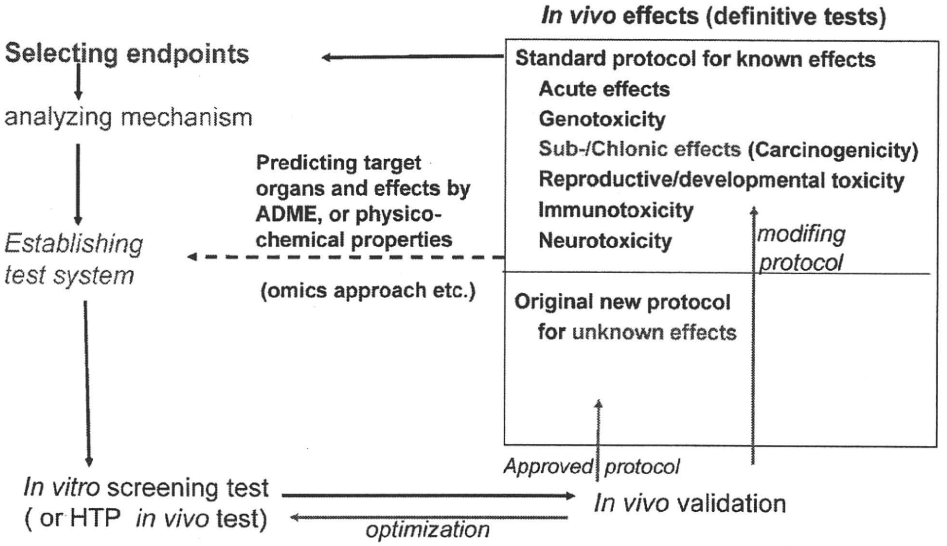

Fig. 4. The Schematic Development of Screening Tests and Definitive Tests

くとも代表的なナノマテリアルによる *in vivo* の慢性影響研究や，その影響を推定するためのナノマテリアルと生体成分との分子レベルでの相互作用や体内残留性様式の解析を進めていくべきであると考えられる．

謝辞 本稿で解説した研究成果の一部は，厚生労働科学研究費補助金（化学物質リスク研究事業）H17-化学-012，H18-化学--一般-007 及び H21-化学--一般-008 の助成によって行われたものです．

REFERENCES

1) Scientific Committee on Emerging and Newly Identified Health Risks, SCENIHR: ⟨http://ec.europa.eu/health/ph_risk/committees/04_scenihr/docs/scenihr_o_003b.pdf⟩, European Commission Web, cited 14 November, 2010.
2) Scientific Committee on Emerging and Newly Identified Health Risks, SCENIHR: ⟨http://ec.europa.eu/health/ph_risk/committees/04_scenihr/docs/scenihr_o_010.pdf⟩, European Commission Web, cited 14 November, 2010.
3) Food Safety Authority of Ireland, FSA, "The Relevance for Food Safety of Applications of Nanotechnology in Food and Feed Industries," Dublin, 2008.
4) UK Committees on Toxicity, Mutagenicity and Carcinogenicity of Chemicals in Food, Consumer Products and the Environment (COT, COM, COC): ⟨http://cot.food.gov.uk/pdfs/cotstatements2005nanomats.pdf⟩, COT Web, cited 14 November, 2010.
5) The Committee on Toxicity of Chemicals in Food, Consumer Products and the Environment: ⟨http://www.food.gov.uk/multimedia/pdfs/cotstatementnanomats200701.pdf⟩, cited 14 November, 2010.
6) Takagi A., Hirose A., Nishimura T., Fukumori N., Ogata A., Ohashi N., Kitajima S., Kanno J., *J. Toxicol. Sci.*, **33**, 105–116 (2008).
7) Sakamoto Y., Nakae D., Fukumori N., Tayama K., Maekawa A., Imai K., Hirose A., Nishimura T., Ohashi N., Ogata A., *J. Toxicol. Sci.*, **34**, 65–76 (2009).
8) Xu J., Futakuchi M., Iigo M., Fukamachi K., Alexander D. B., Shimizu H., Sakai Y., Tamano S., Furukawa F., Uchino T., Tokunaga H., Nishimura T., Hirose A., Kanno J., Tsuda H., *Carcinogenesis*, **31**, 927–935 (2010).
9) Wako K., Kotani Y., Hirose A., Doi T., Hamada S., *J. Toxicol. Sci.*, **35**, 437–446 (2010).
10) Nurkiewicz T. R., Porter D. W., Hubbs A. F., Stone S., Chen B. T., Frazer D. G., Boegehold M. A., Castranova V., *Toxicol. Sci.*, **110**, 191–203 (2009).
11) Ryman-Rasmussen J. P., Cesta M. F., Brody

A. R., Shipley-Phillips J. K., Everitt J. I., Tewksbury E. W., Moss O.R., Wrong B. A., Dodd D. F., Andersen M. E., Bonner J. C., *Nat. Nanotechnol.*, **4**, 747–751 (2009).

12) Shvedova A. A., Kishin E. R., Mercer R., Murray A. R., Johnson V. J., Potapovich A. I., Tyurina Y. Y., Gorelik O., Arepalli S., Schwegler-Berry D., Hubbs A. F., Antonini J., Evans D. E., Ku B. K., Ramsey D., Maynard A., Kagan V. E., Castranova V., Baron P., *Am. J. Physiol. Lung cell. mol. physiol.*, **289**, L698–L708 (2005).

13) Li Z., Hulderman T., Salmen R., Chapman R., Leonars S. S., Young S. H., Shvedova A., Luster M. I., Simeonove P. P., *Environ. Health Perspect.*, **115**, 377–382 (2007).

14) Nemmar A., Hoet P. H., Vandervoort P., Dinsdale D., Nemery B., Hoylaerts M. F., *J. Thromb. Haemost.*, **5**, 1217–1226 (2007).

15) Park E. J., Cho W. S., Jeong J., Yi J., Choi K., Park K., *Toxicology*, **259**, 113–121 (2009).

16) Nygaard U. C., Hansen J. S., Samuelsen M., Alberg T., Marioara C. D., Løvik M., *Toxicol. Sci.*, **109**, 113–123 (2009).

17) Inoue K., Koike E., Yanagisawa R., Hirano S., Nishikwa M., Takano H., *Toxicol. Appl. Pharmacol.*, **237**, 306–316 (2009).

Bull. Natl. Inst. Health Sci., **128**, 27-28 (2010) **Special Report**

レギュラトリーサイエンスにおけるコンピュータを用いた構造活性予測研究の現状と展望

広瀬明彦

Researches on the *in silico* prediction of structure-activity relationship in the regulatory science sectors

Akihiko Hirose

Requirements of *in silico* toxicity prediction system are increasing in the chemical risk assessment fields, as well as in toxicity prediction at the early stage of the new drug development process. Recent amended chemical registration rules require internationally the risk assessment of huge amounts of existing chemicals. The (quantitative) structure-activity relationship ((Q)SAR) models are considered to be most effective tools for the acceleration of toxicity evaluation. In Europe or the United State, several research projects for the development of the (Q)SAR models are ongoing. Following this introduction, four researches on development of *in silico* prediction systems for (Q)SAR in the NIHS are reviewed. These activities must internationally contribute to the integrated chemical risk assessment approaches and/or could assist in the new drug development work.

Keywords: structure-activity relationship, in silico toxicity prediction, risk assessment

コンピュータを用いた（定量的）構造活性相関（(Q)SAR）モデルの発展は，近年のめざましいコンピュータ性能の進化と相俟って，大型コンピュータを必要とした複雑な計算を机上のパーソナルコンピュータで行うことを可能とすると共に，現実的でなかった生体分子の構造や医薬品などの化学物質との原子レベルでの相互作用を解析することが可能となるなど著しいものがある．これらコンピュータを用いた基盤的な（Q)SAR研究の進展は，基礎生物学的な生体反応の解明だけにとどまらず，応用的には特に創薬開発研究などへの貢献が期待されてきていた．一方，このような*in silico*技術は医薬品や環境化学物質と生体との相互作用により引き起こされる有害影響を説明することにも利用できることは明らかであり，近年，医薬品や化学物質の安全性評価を行う研究者や欧米の規制当局側においてリスク評価に有効的なツールとして利用するための試みが活発化してきている．

2007年より施行された欧州の化学品REACH規制（化学物質の登録，評価，許可，制限に関する規則）においては，それまでの既存化学物質や新規化学物質の区別を無くし，年間1トン以上製造または輸入される物質すべてについて登録が義務づけられ，製造・輸入量に応じて要求される毒性情報レベルは異なるものの，2018年までに約3万種といわれる既存化学物質の毒性情報を収集，評価することが求められている．しかし，数万種にも及ぶ化学物質すべてに対して要求される毒性試験を行うことは不可能であることは明らかであり，動物愛護の観点も考慮すると時間と費用を費やしてでも*in vivo*毒性試験を継続していくという選択も，社会的な理解を得ることは困難なところである．一方で，動物実験の代替法としての*in vitro*試験法を開発するための国際的な活動も近年活発化しているが，*in vivo*毒性試験よりスループットが高い*in vitro*試験をもってしても，数万種に及ぶ化合物の実測データを収集することは容易ではなく，しかも多様なエンドポイントをすべて代替するための*in vitro*試験の開発には，まだ相当の時間と技術の向上を必要としている段階である．そのため，類似構造に基づく共通の有害影響の可能性を推定することによるカテゴリーアプローチや（Q)SARモデルの適用は必須のものであると考えられている．欧州ではREACH規則への適用を目指した(Q)SAR研究プロジェクト（ToxTree[1],

To whom correspondence should be addressed:
Akihiko Hirose: 1-18-1 Kamiyoga, Setagaya-ku, Tokyo 158-8501, Japan; Tel: +81-3-3700-9878; Fax: +81-3-3700-1408; E-mail: hirose@nihs.go.jp

OpenTox[2], Caesar Project[3]）が進行しており，これらに市販のDEREKやMultiCASEなどのモデルも取り込んで，既存の毒性試験データベースを基にカテゴリー作成の支援を行うOECD QSAR application toolboxという統合化プラットフォームの開発もOECDのイニシアチブで進行している．米国では，大規模な*in vitro*試験データを基にした毒性予測システムの開発を目指したToxCastプロジェクト[4]などのcomputational toxicologyが進んでいるところである．本特論ではこのような国際的な動向に対応して，国立医薬品食品衛生研究所の４つの部を中心に行われている(Q)SAR研究を紹介する．これらは，現状ではまだ欧米プロジェクト等との直接的な連携は行われていないが，昨年の化審法改正にみられるレギュラトリー分野での国際化に向けて，今後レギュラトリー分野で最も注目される研究分野の一つとなることは疑う余地はない．

1 http://ecb.jrc.ec.europa.eu/qsar/qsar-tools,
2 http://www.opentox.org/,
3 http://www.caesar-project.eu,
4 http://epa.gov/ncct/toxcast/

Desalination 254 (2010) 17–22

Contents lists available at ScienceDirect

Desalination

journal homepage: www.elsevier.com/locate/desal

NF membrane fouling by aluminum and iron coagulant residuals after coagulation–MF pretreatment

Koichi Ohno [a,*], Yoshihiko Matsui [a], Masaki Itoh [b,1], Yoshifumi Oguchi [a], Takuya Kondo [a], Yosuke Konno [a], Taku Matsushita [a], Yasumoto Magara [c,2]

[a] Graduate School of Engineering, Hokkaido University, N13W8, Sapporo 060-8628, Japan
[b] Department of Water Supply Engineering, National Institute of Public Health, Saitama, Japan
[c] Center for Environmental Nano and Bio Engineering, Hokkaido University, Sapporo, Japan

ARTICLE INFO

Article history:
Received 3 August 2009
Received in revised form 15 December 2009
Accepted 17 December 2009
Available online 13 January 2010

Keywords:
Nanofiltration
Microfiltration
Poly-aluminum chloride
Ceramic membrane
Silicate
Potassium

ABSTRACT

The effects of coagulant residuals on fouling of a nanofiltration (NF) membrane were investigated. Experiments were carried out with a laboratory-scale microfiltration (MF)–NF setup and a pilot MF–NF plant. In the laboratory-scale experiments, NF feed water was pretreated with poly-aluminum chloride (PACl) or alum followed by MF. NF membrane permeability declined when the feed water contained residual aluminum at 18 μg/L or more, but not when it was lower than 9 μg/L. When pretreated with ferric chloride, no substantial decline of NF membrane permeability was observed; residual iron did not affect the permeability. When SiO_2 was added to the water before the pretreatment with PACl, the NF membrane permeability declined at about double the speed. Thermodynamic calculations and elemental analysis of foulants recovered from the membranes indicated that the majority of inorganic foulants were compounds composed of aluminum, silicate, and possibly potassium. In the pilot plant, NF feed was pretreated by PACl. Transmembrane pressure for NF doubled over 4.5 months of operation. Although the aluminum concentration in the NF feed was not high (30 μg/L), analysis of membrane foulants revealed excessive accumulation of aluminum and silicate, also suggesting that aluminum residuals caused the membrane fouling by alumino-silicates or aluminum hydroxide.

1. Introduction

Nanofiltration (NF) is a promising advanced drinking water treatment process that offers an efficient alternative to conventional advanced treatment (ozone-activated carbon) and has the potential to produce potable water of better quality. NF is expected to perform better than conventional advanced treatment in removing natural organic matter, precursors of disinfection by-products [1,2] and trace hazardous chemicals such as pesticides [3] from water; however, NF is still more expensive, and its cost needs to be reduced if it is to be widely accepted.

Membrane fouling leads to a continuous decline in membrane permeability, and fouling mitigation considerably reduces the cost of designing and operating membrane filtration systems. In the case of NF of surface waters, the accumulation of particulate matter severely decreases the permeability of the NF membranes; such particulates must be removed by pretreatment processes such as coagulation, followed by clarification and then multi-media filtration or microfiltration (MF).

Although these pretreatments can alleviate the effect of organic foulants as well as that of particulate, the pretreatment increases coagulant residuals to NF feed and they may precipitate on the membrane surface and reduce membrane permeability. Kim et al. [4] used three types of NF feed: untreated raw water (RAW water), pretreated by in-line coagulation followed by MF (MF water) and pretreated by coagulation, sedimentation and sand filtration (CS water). They found that the order of the ratio of inorganic foulants to the total amounts of foulants was CS water>MF water>RAW water. Gabelich et al. tested reverse osmosis (RO) membrane using feed pretreated with conventional or direct filtration treatment plants. They used either alum or ferric chloride, and also used cationic polymer and chloramines for pretreatment. The tests using alum with RO elements revealed rapid deterioration in specific flux, on the other hand, the specific flux using ferric chloride did not decrease over time [5]. They also suggested that three types of aluminum-based foulants: aluminum silicates, aluminum hydroxides, and aluminum phosphates [6]. Accordingly, both pretreatment methods and types of coagulants may play a crucial role in the control of NF/RO fouling. Application of conventional coagulation, clarification and multi-media filtration can

* Corresponding author. Tel./fax: +81 11 706 7282.
E-mail addresses: ohnok@eng.hokudai.ac.jp (K. Ohno), matsui@eng.hokudai.ac.jp (Y. Matsui), itoh@niph.go.jp (M. Itoh), taku-m@eng.hokudai.ac.jp (T. Matsushita), magara@eng.hokudai.ac.jp (Y. Magara).
[1] Tel.: +81 48 458 6298; fax: +81 48 458 6299.
[2] Tel./fax: +81 11 706 7278.

0011-9164/$ – see front matter © 2010 Elsevier B.V. All rights reserved.
doi:10.1016/j.desal.2009.12.020

take advantage of preexisting facilities; however, the processes offset the benefit of small area required for NF membrane process. Pre-coagulated MF would be more advantageous process for pretreatment for NF.

Most of the surface water treatment plants in Japan that have coagulation process currently use aluminum coagulants [7]. During our pilot plant experiment [8], which is also discussed in this study, we found that residual aluminum coagulants in the NF feed might cause the membrane fouling. Therefore, the objective of this study was to investigate the effects of coagulant residuals on NF membrane fouling when NF is applied as an advanced water treatment process of surface or ground water. In laboratory-scale experiments, we used two types of aluminum coagulant: poly-aluminum chloride (PACl) and alum and pretreated by in-line coagulation and ceramic MF. As an alternative coagulant, iron coagulant (ferric chloride) was also used. To clarify the effect of residual coagulants, groundwater that contained low organic matter was used as raw experimental water. To elucidate the effects of SiO_2 on the NF membrane fouling, we added SiO_2 to the raw water in some of the experiments. The results of the pilot scale experiment, in which PACl was used as a coagulant agent, were also presented and discussed.

2. Experimental

2.1. Laboratory-scale experiment

In the laboratory-scale experiment, Hokkaido University groundwater was used as raw experimental water. The average quality of this water was: DOC 0.5 mg/L, EC 450 μS/cm, pH 7.2, Na 29 mg/L, K 9.6 mg/L, Ca 50 mg/L, Mg 15 mg/L, Cl 25 mg/L, SO_4 40 mg/L. Types of coagulants used were PACl (10% Al_2O_3, basicity 52%, Japanese Industrial Standard (JIS) grade), alum (Aluminum Sulfate 14–18 Water, reagent grade, Wako Pure Chemicals, Osaka, Japan) or ferric chloride (Iron (III) Chloride Hexahydrate, reagent grade, Wake Pure Chemicals). The raw water was firstly treated with activated carbon cartridge filter to quench residual chlorine and then pretreated by in-line coagulation followed by MF. The MF filtrate (pH 7.0–7.1) was then pumped at a rate of 1.5 L/h to a flat sheet membrane test cell (filtration area 60 cm^2, C10-T, Nitto Denko Matex Corp., Tokyo, Japan; Fig. 1) that housed the NF membrane (UTC-60, nominal NaCl rejection 55%, Toray Industries, Inc.). NF was performed at a filtration flux of 2.5 cm/h and a water recovery rate of 10%. The system flow is shown in Fig. 2. We conducted nine experimental runs and their conditions are summarized in Table 1. In all experimental runs, the coagulant dose was set at 0.04 mM (1.1 mg-Al/L, 2.2 mg-Fe/L). MF was performed with a laboratory-use ceramic membrane (nominal pore size 0.1 μm, membrane area 0.4 m^2, NGK Insulators, Nagoya, Japan) at very low filtration flux (0.83 cm/h), without periodic hydraulic backwashing; the MF membrane was replaced with a chemically cleaned membrane when the inlet pressure reached 0.05 MPa. After the NF experiments, spent NF membranes were cleaned with 2% citric acid, and the aluminum and iron concentrations in the citric acid drain were analyzed.

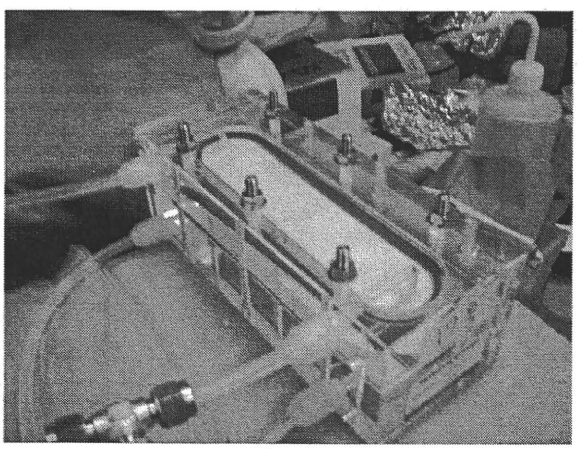

Fig. 1. Flat sheet membrane test cell.

After five experimental runs with the laboratory-scale experimental setup, an automatic hydraulic backwash system was introduced to the MF step; the MF was performed at a normal filtration flux (6.25 cm/h), and the MF membrane was hydraulically cleaned by backwash at a pressure of 500 kPa for 10 s every 2 h [9]. MF permeate (pH 6.8–7.0) was introduced to the NF membrane test cell at a filtration flux of 2.08 cm/h, which is slightly lower than the fluxes used for the previous experiments. Runs 6–9 were conducted with this system. Run 6 used PACl as a coagulant, and Run 7 used ferric chloride.

In the next two experimental runs (Runs 8 and 9), SiO_2 was added to the chlorine-quenched groundwater before coagulation with PACl and MF pretreatment. By comparing these results with the results of Run 6, in which the mean silicate concentration was 35 mg-SiO_2/L, we investigated the effect of silicate on the NF membrane fouling. Diluted sodium silicate was added so that the silicate concentration in the NF feed would be approximately 80 mg-SiO_2/L. Sodium silicate is a basic reagent, and thus the pH was adjusted to approximately 7 with hydrochloric acid. After Runs 6, 8, and 9, the spent NF membranes were cleaned sequentially with HCl, NaOH, and citric acid; and then the aluminum, silicate, calcium, and potassium concentrations in the cleaning water were analyzed.

2.2. Pilot MF–NF plant experiment

The pilot plant received water at a rate of 24 m^3/h from the outlet of a sedimentation basin of the Ishikawa Water Treatment Plant, Okinawa, Japan, after PACl (basicity 50%, JIS grade) coagulation. In the pilot plant, MF (polyvinylidene fluoride membrane, nominal pore size 0.1 μm; Toray Industries, Inc., Tokyo, Japan) filtrates (pH 6.5–7.3) were transferred to the NF modules (nominal NaCl rejection 55%; polyamide SU-610, Toray Industries, Inc.), which were operated at constant flux (2.5 cm/h) and water recovery rate (95%) by adjustment of the feed pressure. Average quality of MF filtered water was: TOC 0.9 mg/L, EC 185 μS/cm, Na 19 mg/L, Ca 11 mg/L, Cl 27 mg/L, SO_4 14 mg/L, and residual Al was 0.03 mg/L. The 15 NF modules were placed in a multistage array (8, 4, 2, and 1 modules in series), and the water recovery rate of each element was about 13%. Details of the process configuration and operation are given elsewhere [8]. After 4.5 months of system operation, foulants on the NF membrane surface were collected by gentle scraping of the membrane deposits. The foulants were then dried, weighed, combusted for 30 min in a muffle furnace at 550 °C, and then weighed again to obtain the mass of fixed solid. The recovered foulant was analyzed for Al, Ca, Fe, S, and Si.

2.3. Analytical methods

Aluminum and iron concentrations were measured by an inductively coupled plasma-mass spectrometer (ICP-MS; HP-4500; Agilent Technologies, Inc., Palo Alto, CA, USA). Ion concentrations (Na^+, K^+, Mg^+, Ca^+, Cl^-, NO_3^-, SO_4^{2-}) were measured by ion chromatograph (DX-120, Nippon Dionex K.K., Osaka, Japan). SiO_2 was measure by molybdenum yellow colorimetric method. TOC and DOC were measured by TOC-5000A (Shimadzu Corporation, Kyoto, Japan) or Sievers 900 Laboratory TOC analyzer (GE Analytical Instruments, Boulder, CO, USA).

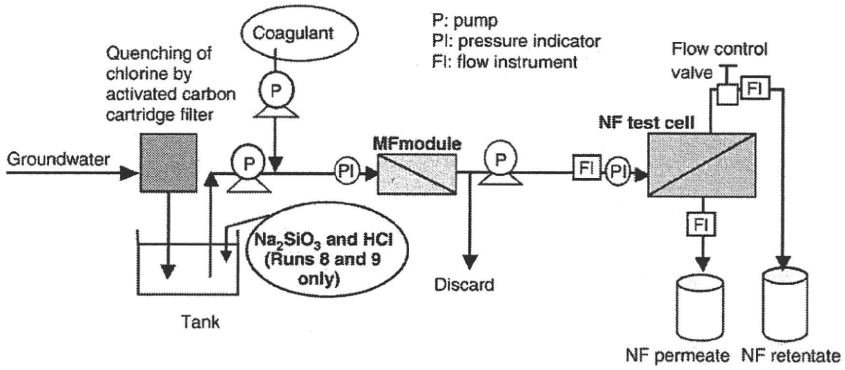

Fig. 2. Experimental setup for laboratory-scale MF–NF experiments.

3. Results and discussion

3.1. Laboratory-scale experiment pretreated with aluminum coagulants (Runs 1–3)

Changes in NF membrane permeability over time in the laboratory-scale experiment with different aluminum coagulants (i.e., PACl and alum) are compared in Fig. 3. Because variation in the initial filtration flux of the pieces of NF membrane sheet used in the NF cross-flow cell was small, nanofilter permeability was evaluated in terms of the dimensionless standardized filtration flux, which is the standardized flux at 1 MPa and 25 °C divided by the standardized flux for pure water, as described by the following equations [10]:

$$J = \frac{Q}{A} \cdot \frac{\alpha}{\Delta P} \tag{1}$$

where J is standardized filtration flux [m/(h MPa)], Q is filtration rate (m^3/h), A is membrane surface area (m^2), α is a temperature compensation factor to 25 °C, and ΔP is transmembrane pressure (TMP) (MPa); and

$$J^* = \frac{J}{J_W} \tag{2}$$

where J^* is dimensionless standardized flux, and J_W is standardized filtration flux for pure water [m/(h MPa)].

After 25 days of operation of the laboratory-scale experiment with PACl coagulant (Run 1) in which MF permeate (NF feed) had a mean aluminum concentration of 20 μg/L, the filtration flux decreased by about 15% (Fig. 3). In an experiment with alum coagulant (Run 2) in which NF feed contained aluminum at a mean concentration of 18 μg/L, the filtration flux again decreased by about 15%. Lower mean aluminum concentration (8.7 μg/L) in NF feed was observed in another experiment with PACl coagulant (Run 3); we did not change any specific condition of coagulation and MF, and we could not elucidate the reason why we could achieve this lower residual aluminum concentration. In this Run 3, the NF membrane permeability did not change substantially. The percentage rejection of aluminum by NF was more than 85%; most of the aluminum remaining after MF obviously could not permeate the NF membrane and thus had the potential to be deposited on the NF membrane, reducing membrane permeability. However, the aluminum concentrations in the NF retentates were only slightly higher than the concentrations in the corresponding NF feed; more than 98% of the aluminum fed to the NF was discharged with the NF retentate. Therefore, the high rejection ratio of aluminum did not produce a retentate that was highly concentrated in comparison with the feed and did not necessarily result in a high deposition rate on the NF membrane.

Table 1
Laboratory-scale experimental conditions and mean concentrations of residual coagulant in NF feed water.

Run	Type of coagulant	Automatic backwash system in MF and filtration flux (cm/h)	SiO_2 was added to be ~80 mg/L.	Mean concentration of residual coagulant in NF feed water	NF filtration flux (cm/h)
1	PACl	No (0.83)		20 μg-Al/L	2.5
2	Alum	No		18 μg-Al/L	2.5
3	PACl	No		8.7 μg-Al/L	2.5
4	$FeCl_3$	No		10 μg-Fe/L	2.5
5	$FeCl_3$	No		18 μg-Fe/L	2.5
6	PACl	Yes (6.25)		40 μg-Al/L	2.08
7	$FeCl_3$	Yes		8.6 μg-Fe/L	2.08
8	PACl	Yes	Yes	103 μg-Al/L	2.08
9	PACl	Yes	Yes	85 μg-Al/L	2.08

3.2. Laboratory-scale experiment with iron coagulant pretreatment (Runs 4 and 5)

Unlike Runs 1 and 2, Runs 4 and 5 did not show a large change in nanofilter permeability (Fig. 4). Mean iron concentrations in the NF feed after the ferric chloride coagulation and MF pretreatments in Runs 4 and 5 were 10 and 18 μg/L, respectively, and the aluminum concentration in the NF feeds was less than 2 μg/L. The percentage rejection of iron by NF was 60–90%, which was not as high as that of aluminum. These results suggest that the concentration of residual aluminum after coagulation influenced NF fouling more strongly than did the residual iron concentration.

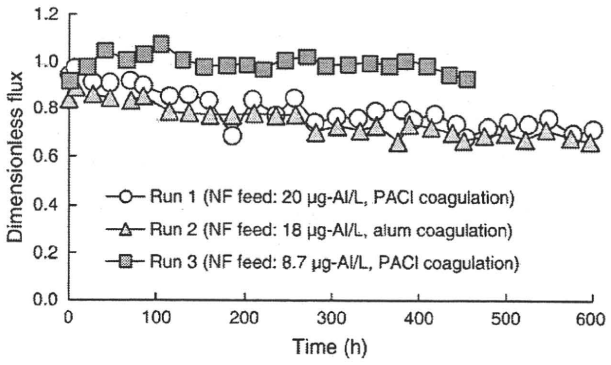

Fig. 3. Time dependence of dimensionless standardized flux (standardized flux/standardized flux for pure water) for NF after coagulation and MF in the laboratory-scale experiment (Runs 1–3).

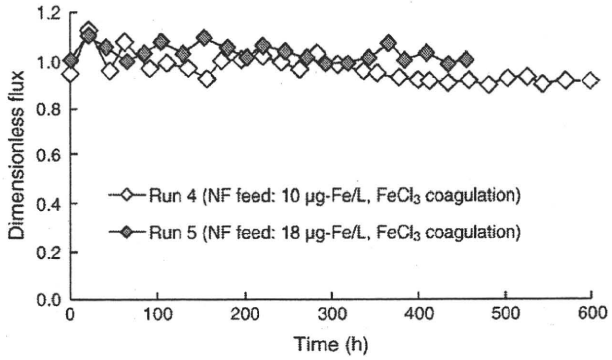

Fig. 4. Time dependence of dimensionless standardized flux (standardized flux/standardized flux for pure water) for NF after coagulation and MF in the laboratory-scale experiment (Runs 4 and 5).

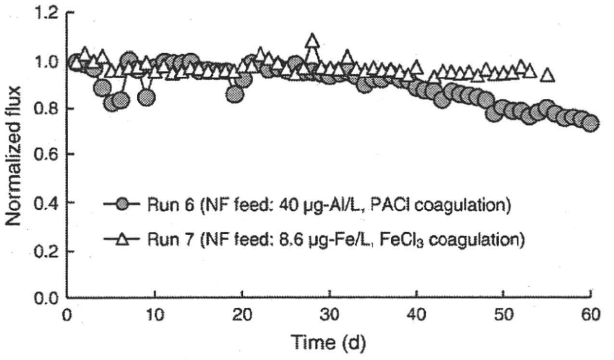

Fig. 5. Time dependence of normalized flux (standardized flux/first day standardized flux) for NF after coagulation and MF in the laboratory-scale experiment (Runs 6 and 7).

Table 2 summarizes the masses of aluminum and iron eluted from the spent NF membranes by citric acid. The membranes used in Runs 1 and 2, which showed larger permeability declines, contained more aluminum (3.6 and 4.0 mg/m^2-membrane surface) than the others. The amount of iron eluted from the spent membranes was similar to the amount of aluminum (Table 2), but unlike the mass of aluminum, the mass of iron was not obviously correlated with membrane permeability decline (Figs. 3 and 4).

3.3. Laboratory-scale experiment with backwashing in the MF step

3.3.1. Comparison of aluminum and iron coagulation (Runs 6 and 7)

An automatic backwash was introduced to the MF step after Run 5, and this alteration permitted MF at a normal filtration flux. Under this altered condition, experimental runs with PACl coagulant (Run 6) and ferric chloride (Run 7) were performed. Nanofilter permeability declined during Run 6 (Fig. 5). In this run, the NF feed contained residual aluminum of 40 μg/L in average, and the membrane permeability declined by 25% after 60 days (1440 h) of operation. The permeability declined at lower rates in this run than in Runs 1 and 2; this result was probably due to the fact that the filtration flux (2.08 cm/h) was lower than in Runs 1 and 2 (2.5 cm/h). In the experiment with ferric chloride (Run 7), no substantial decline in NF membrane permeability was observed; this result was the same as those for Runs 4 and 5.

3.3.2. Effect of SiO_2 addition (Runs 6, 8 and 9)

When SiO_2 was added to the water before the pretreatment by coagulation with PACl and MF (Runs 8 and 9), the NF membrane permeability declined at about double the speed observed for Run 6 (Fig. 6). The pH in Run 8 was not strictly controlled (the pH of the NF feed water fluctuated between 6.6 and 7.5). Aluminum is more soluble at alkaline pH than at neutral pH [11], and therefore the mean aluminum concentration in the NF feed was as high as 103 μg/L. In Run 9, the pH was controlled more strictly (6.7–7.0 over the course of the run); nevertheless, the mean aluminum concentration was also rather high (85 μg/L) in this run. This higher residual aluminum may have been due to the effect of excess silicate. Lartiges et al. [12] reported that flocculation of colloidal silica with polymerized aluminum begins with the formation of negatively charged aluminosilicate sites. Duan and Gregory [13,14] investigated the interaction of aluminum coagulants with silica and found that a small amount of dissolved silica can improve coagulation by affecting the charge-neutralizing behavior of hydrolyzed aluminum species, but silica coagulation is inhibited as the amount of silica is increased, as a result of the increasing negative charge of the particles.

Table 2
NF membrane foulants in the laboratory-scale MF–NF experiment in Runs 1–5.

	Coagulant	Foulant	
		Al (mg/m^2)	Fe (mg/m^2)
Run 1	PACl	3.6	2.5
Run 2	Alum	4.0	1.7
Run 3	PACl	1.8	2.1
Run 4	$FeCl_3$	0.2	3.3
Run 5	$FeCl_3$	1.2	1.8

To explore further the effect of a large amount of silicate on the faster decline of NF membrane permeability, we cleaned the spent membrane sequentially with HCl, NaOH, and citric acid after the experimental runs. Results after chemical cleaning with HCl are shown in Table 3; aluminum and silicate were recovered in molar ratios of 1:0.49 (Run 6), 1:1.52 (Run 8), and 1:1.78 (Run 9). These results suggest that aluminum and silicate were major inorganic foulants of the nanofilter.

We calculated the aluminum solubility diagram for the NF feed solution used in Runs 6, 8, and 9 (Fig. 7) with Geochemist's Workbench (ver. 6, RockWare, Inc., Golden, CO, USA). The major difference in the feed water quality of these runs was silicate concentration. The aluminum concentration in the NF feed water exceeded the upper solubility limit in the case of gibbsite ($Al(OH)_3$), pyrophyllite ($AlSi_2O_5OH$), and kaolinite ($Al_2Si_2O_5(OH)_4$), that is, an aluminum compound and two compounds containing both aluminum and silicate. Furthermore, changing the silicate concentration from 40 to 80 mg-SiO_2/L led to a large decrease in the solubility of pyrophyllite and kaolinite (from dotted line to solid line), although the solubility of gibbsite did not change. This result implies that more aluminum silicate compounds may have deposited on the NF membrane as the amount of silicate in the feed water increased. Therefore,

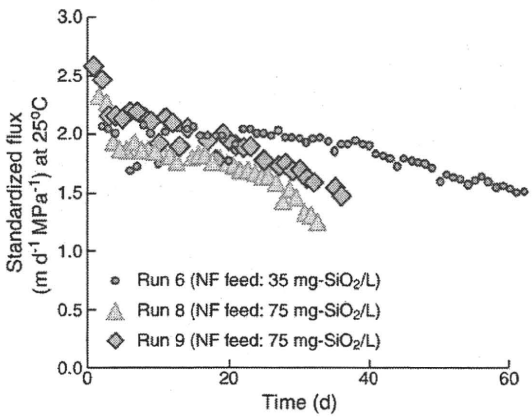

Fig. 6. Changes in standardized flux for NF after coagulation and MF in the laboratory-scale experiment (Runs 6, 8, and 9).

Table 3
Molar ratio of Si and K to Al recovered by cleaning with HCl.

	Mean Si concentration in NF feed water (mg-SiO_2/L)	Si/Al (mol/mol)	K/Al (mol/mol)
Run 6	35	0.49	0.48
Run 8	75	1.52	1.02
Run 9	77	1.78	0.70

the silicate concentration could play a major role in NF membrane fouling, even though the rejection rate of silicate itself was not high: the rejection percentages of silicate were only 10–20% in both the pilot plant and laboratory experiments.

Calcium was not detected on the spent membrane from Run 6 but was detected in Runs 8 and 9. In these runs, calcium was detected in the NaOH cleaning solution, which suggests that calcium fouled the NF membrane in combination with organic substances. In contrast, potassium was largely detected in the HCl and citric acid cleaning solutions. The molar ratios of aluminum to potassium in the HCl cleaning solution were 1:0.48 (Run 6), 1:1.02 (Run 8), and 1:0.70 (Run 9) (Table 3). The thermodynamic calculation (Geochemist's Workbench) also suggests that the aluminum concentration in the NF feed water was higher than the solubility of mordenite-K ($K_2Al_2Si_{10}O_{24}\cdot 7H_2O$) (Fig. 7), and in some calculations, clinoptilolite-K ($K_6Al_6Si_{30}O_{72}$) also appeared as a candidate foulant (data not shown). These two minerals are siliceous zeolites [15,16], and the chemical formulas of natural zeolites are very complicated; not only potassium but also other cations, including sodium, calcium, and magnesium, are incorporated into the zeolites because zeolites have ion-exchange properties [17]. The foulants in the other experiments were not analyzed for potassium (because we did not consider potassium as a potential foulant when the research started) and other cations except calcium; we therefore could not elucidate further the effects of these cations.

3.4. Pilot MF–NF plant experiment

The permeability of the first stage modules in the multistage array of nanofilters declined with operation time (Fig. 8). Although no severe membrane fouling was expected for the first stage module, TMP doubled and the permeability (represented by standardized filtration flux at 25 °C and 1 MPa) was reduced to 1/3 the original permeability over 4.5 months of operation. The mean silt density index of the NF feed water was 2.25 (minimum 1.0, maximum 3.2), which suggests an absence of severe fouling by particulate matter. Gabelich et al. [18] recently reported that aluminum residuals, most

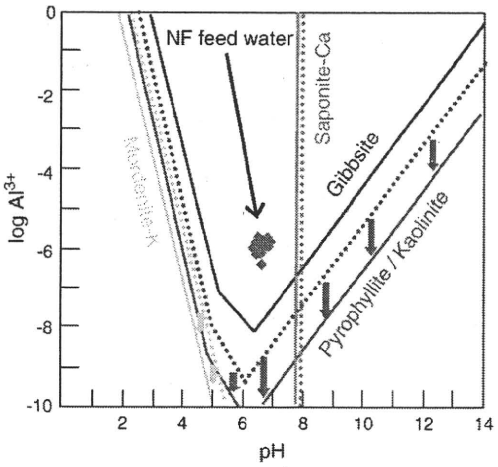

Fig. 7. Solubility diagram for aluminum at 25 °C: dotted lines, solubility diagram for the NF feed solution in Run 6 (40 mg-SiO_2/L); solid lines, Runs 8 and 9 (80 mg-SiO_2/L).

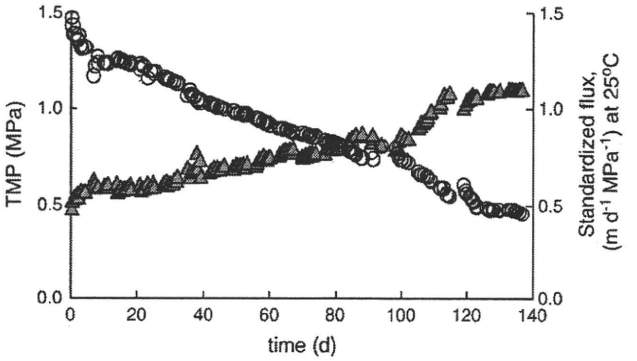

Fig. 8. Water permeability for the first stage of the multistage array in the NF pilot plant. Triangles, transmembrane pressure (TMP); circles, permeability represented by standardized filtration flux at 25 °C and 1 MPa of TMP.

notably from alum coagulation, cause colloidal fouling of RO membranes through interaction with the ambient silica to form aluminum silicate. They suggested that keeping the aluminum concentration at <50 μg/L would result in stable RO membrane performance. The aluminum concentration in the NF influent of our experiment was below this suggested limit (mean 30 μg/L, minimum 10 μg/L, maximum 47 μg/L).

Collection of the membrane deposits was followed by combustion at 550 °C, and we recovered remaining foulants (regarded as ash) at a rate of 330 mg/m^2-membrane surface. We conducted elemental analysis of this ash for Al, Ca, Fe, S, SiO_2 and their concentrations were 46, 0.33, 2.5, 3.9, and 30 mg/m^2, respectively. This excessive accumulation of aluminum and silicate also suggests that aluminum residuals probably caused the membrane fouling by forming alumino-silicates or aluminum hydroxide.

4. Conclusion

Residual aluminum in the NF feed water greatly increased the decline of NF membrane permeability both in a pilot MF–NF plant experiment and in laboratory-scale MF–NF experiments when aluminum coagulants were used in the pretreatment process. On the contrary, there was no substantial decline in NF membrane permeability in the laboratory-scale experiments when ferric chloride was used as a coagulant. In the laboratory-scale experiments with aluminum coagulants, NF membrane permeability declined when the feed water contained residual aluminum at 18 μg/L or more, but not when the aluminum concentration was lower than about 9 μg/L. Therefore, the control of residual aluminum in the pretreatment processes of NF is crucial for mitigation of severe fouling of the NF membrane. The silicate concentration in the NF feed water also greatly increased NF membrane fouling, and other cations, especially potassium, may have been incorporated in the foulants in the form of zeolites.

References

[1] M. Siddiqui, G. Amy, J. Ryan, W. Odem, Membranes for the control of natural organic matter from surface waters, Water Res. 34 (13) (2000) 3355–3370.
[2] I. Mijatovic, M. Matosic, H. Cerneha, D. Bratulic, Removal of natural organic matter by ultrafiltration and nanofiltration for drinking water production, Desalination 169 (2004) 223–230.
[3] B. Van der Bruggen, J. Schaep, W. Maes, D. Wilms, C. Vandecasteele, Nanofiltration as a treatment method for the removal of pesticides from ground waters, Desalination 117 (1998) 139–147.
[4] H.A. Kim, J.H. Choi, S. Takizawa, Comparison of initial filtration resistance by pretreatment processes in the nanofiltration for drinking water treatment, Sep. Purif. Technol. 56 (2007) 354–362.
[5] C.J. Gabelich, T.I. Yun, B.M. Coffey, I.H. Suffet, Effects of aluminum sulfate and ferric chloride coagulant residuals on polyamide membrane performance, Desalination 150 (2002) 15–30.

[6] C.J. Gabelich, W.R. Chen, T.I. Yun, B.M. Coffey, I.H. Suffet, The role of dissolved aluminum in silica chemistry for membrane processes, Desalination 180 (2005) 307–319.
[7] K. Ohno, E. Kadota, Y. Matsui, Y. Kondo, T. Matsushita, Y. Magara, Plant capacity affects some basic indices of treated water quality: multivariate statistical analysis of drinking water treatment plants in Japan, J. Water Supply Res. T. AQUA 58 (7) (2009) 476–487.
[8] T. Ohgai, Y. Oguchi, K. Ohno, T. Kamei, Y. Magara, M. Itoh, Development of evaluation methods to introduce a nanofiltration membrane process in drinking water treatment, Water Sci. Tech. Water Supply 6 (2) (2006) 9–17.
[9] Y. Matsui, H. Hasegawa, K. Ohno, T. Matsushita, S. Mima, Y. Kawase, T. Aizawa, Effects of super-powdered activated carbon pretreatment on coagulation and trans-membrane pressure buildup during microfiltration, Water Res. 43 (20) (2009) 5160–5170.
[10] M. Itoh, S. Kunikane, Evaluation method of nanofiltration membranes by semibatch experiment, J. Jpn. Water Works Assoc. 68 (11) (1999) 21–31 (in Japanese).
[11] MWH, Water Treatment: Principles and Design2nd ed, John Wiley & Sons, Inc, Hoboken, New Jersey, 2005.
[12] B.S. Lartiges, J.Y. Bottero, L.S. Derrendinger, B. Humbert, P. Tekely, H. Suty, Flocculation of colloidal silica with hydrolyzed aluminum: an 27Al solid state NMR investigation, Langmuir 13 (1997) 147–152.
[13] J. Duan, J. Gregory, Influence of soluble silica on coagulation by aluminium sulphate, Colloid. Surface A 107 (1996) 309–319.
[14] J. Gregory, J. Duan, The effect of dissolved silica on the action of hydrolysing metal coagulants, Water Sci. Tech. 38 (6) (1998) 113–120.
[15] K. Itabashi, T. Fukushima, K. Igawa, Synthesis and characteristic properties of siliceous mordenite, Zeolites 6 (1986) 30–34.
[16] D. Zhao, K. Cleare, C. Oliver, C. Ingram, D. Cook, R. Szostak, L. Kevan, Characteristics of the synthetic heulandite–clinoptilolite family of zeolites, Micropor. Mesopor. Mat. 21 (1998) 371–379.
[17] R.Y. Ning, Discussion of silica speciation, fouling, control and maximum reduction, Desalination 151 (2002) 67–73.
[18] C.J. Gabelich, K.P. Ishida, F.W. Gerringer, R. Evangelista, M. Kalyan, I.H. Suffet, Control of residual aluminum from conventional treatment to improve reverse osmosis performance, Desalination 190 (2006) 147–160.

Geosmin and 2-methylisoborneol adsorption on super-powdered activated carbon in the presence of natural organic matter

Y. Matsui, Y. Nakano, H. Hiroshi, N. Ando, T. Matsushita and K. Ohno

ABSTRACT

Geosmin and 2-methylisoborneol (2-MIB) are naturally occurring compounds responsible for musty-earthy-odors in surface water supplies. They are a severe problem confronting utilities worldwide. Adsorption by powdered activated carbon (PAC) is a widely used process to control this problem, but it has low efficiency, which engenders large budget spending for utilities services. Super-powdered activated carbon (S-PAC) is activated carbon with much finer particles than those of PAC. Experiments on geosmin and 2-MIB adsorptions on S-PAC and PAC were conducted. Geosmin and 2-MIB adsorption capacities on S-PAC were not smaller than those on PAC although natural organic matter, which adversely impacted the adsorption capacity of geosmin and 2-MIB, was more adsorbed on S-PAC than on PAC, meaning that the adsorption competition is less severe for S-PAC than for PAC.

Key words | competitive adsorption, humic substance, PAC, particle size, submicrometer, taste and odor

Y. Matsui (corresponding author)
Y. Nakano
H. Hiroshi
N. Ando
T. Matsushita
K. Ohno
Graduate School of Engineering,
Hokkaido University,
N13W8,
Sapporo 060-8628,
Japan
E-mail: *matsui@eng.hokudai.ac.jp*

INTRODUCTION

Although taste and odor problems are not considered a direct threat to public health, they are perhaps the single greatest public relations issue confronting many water utilities because consumers generally rely on the taste of their water as the primary indicator of its safety (Wear 2006). Taste and odor are aesthetic qualities of drinking water. For that reason, their assessment depends on human perception. The human perception of taste and odor in drinking water depends on numerous factors, but tastes and odors are sometimes perceived at extremely low concentrations, typically for taste and odor problems caused by algae, mold, and bacteria. The major components within algae that give rise to tastes and odors are geosmin and 2-MIB. In Japan, geosmin and 2-MIB concentrations in tap water from drinking water suppliers are regulated by the drinking water quality standard to be less than 10 ng/L, which are the lowest concentrations among all items.

doi: 10.2166/wst.2010.415

The removal of geosmin and 2-MIB during water treatment is usually done by adsorption using activated carbon or oxidation by ozone. Among such methods, PAC is the simplest most widely applied method, but means that are more economical are anticipated (Newcombe & Cook 2002). The process of 2-MIB and geosmin adsorption onto PAC takes time, usually more than 1 h (Huang *et al.* 1996). Maximizing the contact time between PAC and water is critical, for efficiently utilize its adsorptive capacity of the PAC. Particle size reduction of PAC, which improves the adsorbate uptake rate, is another means for efficient utilization of its adsorptive capacity (Najm *et al.* 1990). Recently, activated carbon that is much finer than conventional PAC has become available: super-powdered activated carbon (S-PAC). In fact, S-PAC is far superior to PAC in removing geosmin and natural organic matter (NOM) (Matsui *et al.* 2004, 2007, 2009). However, the removal of 2-MIB, which has less affinity to activated

carbon than geosmin, has not yet been investigated. Moreover, characteristics of adsorptive removals of 2-MIB/geosmin by S-PAC, which adsorbs NOM more than PAC, remain unknown. In this paper, the adsorption equilibrium of 2-MIB/geosmin on S-PAC and PAC were investigated experimentally along with their adsorption in the presence of NOM.

METHODS

Activated carbon

Commercially available wood-based PAC (Taikou-W; Futamura Chemical Industries Co. Ltd., Gifu, Japan) was wet-ground to produce S-PAC using a wet bead mill (Metawater Co. Ltd.; Tokyo, Japan, Matsui *et al.* 2004). We used both the S-PAC and the as-received (i.e. normal) PAC. The S-PAC was stored in slurries (2.1 and 0.21%) with pure water at 4°C, as was the PAC (2.6 and 0.28%). The particle size distributions of S-PAC and PAC (Figure 1) were determined using laser-light scattering instruments (LMS-300; Seishin Co., Ltd., Tokyo, Japan).

Water samples

Hakucho and Suwannee humic acid waters were used as source waters containing NOM. The Hakucho water samples were collected from Lake Hakucho in Hokkaido, Japan, transported in polyethylene tanks, and stored at 4°C. The TOC and ultraviolet absorbance at 260 nm (UV260) served as parameters for bulk NOM quantification

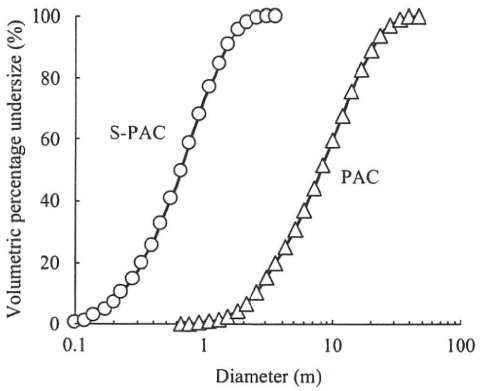

Figure 1 | Particle size distributions of S-PAC and PAC.

(TOC: Model 810; Sievers Instruments, Inc., Boulder, CO, USA; UV260: Model UV-240, Shimadzu Corp., Kyoto, Japan). The Suwannee humic acid water was prepared by dissolving Suwannee humic acid (International Humic Substance Society) in pure water (Milli-Q Advantage, Millipore Co.) after inorganic ions, which bring the ionic composition equal to that of water from Hakucho water. The molecular weight (MW) distributions of NOMs in the Hakucho water and Suwannee humic acid water were determined using liquid chromatography–organic carbon detection [HP1100 (Agilent Technologies, Inc., CA, USA); packed column GL-P252 (Hitachi, Ltd.); eluent: 0.02 M Na_2HPO_4 + 0.02 M KH_2PO_4]. Polystyrene sulfonate (MW 1800, 4600, and 8000) was used for calibration. The UV absorbance at 260 nm and TOC (Model 810 Turbo; GE Analytical Instruments) of the column effluent were measured continuously (see Table 1).

Single solute solutions of geosmin and 2-MIB were prepared respectively by diluting geosmin-MeOH liquid (Supelco, Sigma Aldrich Japan, Tokyo) and 2-MIB-MeOH liquid (Supelco, Sigma-Aldrich Japan, Tokyo) with pure water (Milli-Q Advantage, Millipore Corp., Billerica, MA, USA). Solutions of geosmin and 2-MIB in natural water were prepared respectively by diluting geosmin (Wako Pure Chemical Industries, Ltd., Osaka, Japan) and 2-MIB (Wako Pure Chemical Industries, Ltd., Osaka, Japan) with pure water and natural water (Hakucho water or Suwannee humic acid water). All waters were filtered through a 0.2 μm pore size membrane before use. Geosmin and 2-MIB concentrations were adjusted to 100 ng/L. Geosmin and 2-MIB concentrations were analyzed using a Thermal Desorption System (TDS), a gas chromatography/mass spectrometer) (GC/MS), and the Stir Bar Sorptive Extraction (SBSE) method (Gerstel GmbH and Co. KG, Tokyo, Japan, and Agilent Technologies Japan, Tokyo) using deuterium-labeled geosmin (Hayashi Pure Chemical Ind., Ltd., Osaka, Japan) as an internal standard, or using a Purge and Trap Concentrator Coupled to the GC-MS (GCMS-QP2010 Plus; Shimadzu Corp., Kyoto, Japan; Aqua PT 5000 J, GL Sciences Inc., Tokyo, Japan).

Table 1 | Properties of natural water samples

	Hakucho water	Suwannee humic acid water
TOC	1.4 mg/L	1.6 mg/L
UV260	0.028 cm^{-1}	0.096 cm^{-1}

Batch adsorption tests

In adsorption equilibrium tests, aliquots (125 mL) from the 1 L solution containing each geosmin/2-MIB and PAC were transferred to 125-mL vials. Then the vials were agitated on a shaker for one week. In the preliminary experiment, it was confirmed that in one week geosmin/2-MIB adsorption equilibrium was reached and NOM adsorption equilibrium was almost reached.

After the water samples were filtered through a 0.2-μm membrane filter (DISMIC-25HP; Toyo Roshi Kaisha, Ltd., Tokyo), the water-phase of each geosmin/2-MIB concentration was measured using TDS-GC/MS and SBSE. The solid-phase of each geosmin/2-MIB concentration was calculated from the mass balance. They are shown against water-phase concentrations to obtain isotherm data. In the natural water system, the NOM concentration was evaluated by measuring the total organic carbon (TOC) concentration (Sievers 900 Laboratory TOC Analyzer; GE Analytical Instruments, Boulder, Colorado, USA).

RESULTS AND DISCUSSION

Geosmin and 2-MIB adsorption capacities of S-PAC and PAC

As presented in Figure 2, no large difference in geosmin adsorption capacity was observed between S-PAC and PAC although there was a tendency observed that adsorption

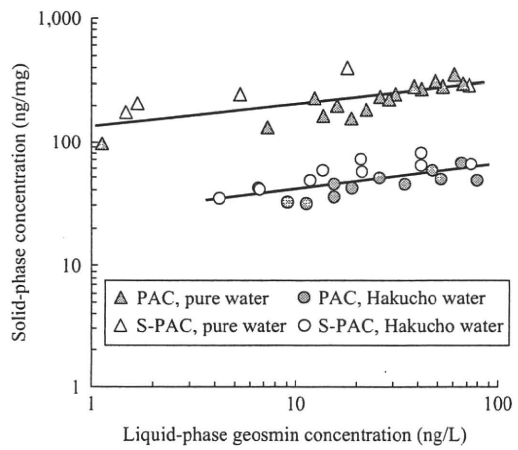

Figure 2 | Adsorption isotherms of geosmin in Hakucho water and pure water (the lines are Freundlich model fits).

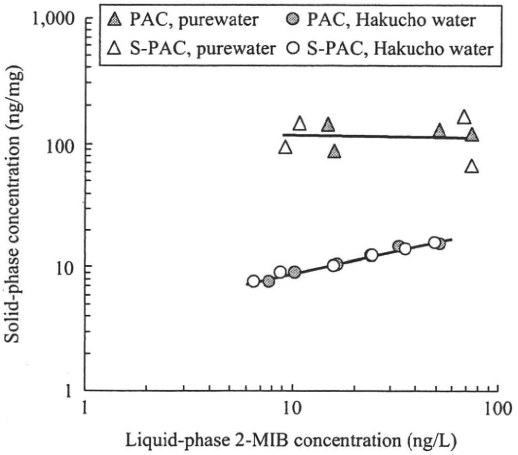

Figure 3 | Adsorption isotherms of 2-MIB in Hakucho water and pure water (the lines are Freundlich model fits).

capacity on S-PAC was slightly higher than on PAC. For 2-MIB, adsorption capacities were not clearly different between S-PAC and PAC, as shown in Figure 3. In contrast, for NOM, a higher adsorption capacity of S-PAC than on PAC was reported for natural organic matter (Matsui *et al.* 2004). The reason for the higher NOM adsorption capacity on S-PAC was not clear, but the effect of carbon particle size on the adsorption capacity differed depending on the adsorbates. Adsorption equilibrium data of Figure 2 also show that the geosmin adsorption capacity was smaller in natural water than in pure water. This resulted from adsorption competition between NOM and geosmin, where NOM reduced the adsorption capacity of geosmin. The extents of geosmin adsorption capacity reductions were similar between S-PAC and PAC. The geosmin adsorption capacity was also almost the same for S-PAC and PAC in the presence of NOM. Figure 4 shows adsorption isotherms of NOM in the presence of geosmin for S-PAC and PAC in terms of TOC. For both Hakucho water and Suwannee humic acid water, S-PAC showed higher NOM adsorption capacity than PAC, indicating that S-PAC adsorbed NOM more than PAC at a given dose. The geosmin adsorption capacity in natural water did not, however, differ between S-PAC and PAC. The geosmin adsorption capacity on S-PAC was decreased by the competitive effects of NOM, but the competitive effects are the same degree between S-PAC and PAC although S-PAC adsorbed the larger amount of NOM than PAC. In other words, the large amount of NOM adsorbed onto S-PAC exerted the same

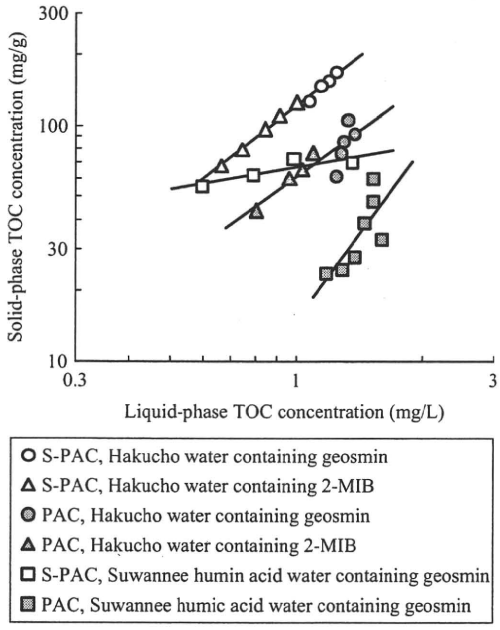

Figure 4 | TOC adsorption isotherms in Hakucho water and Suwannee humic acid water (the lines are Freundlich model fits).

degree of competition to geosmin adsorption as the small amount of NOM adsorbed onto PAC. A similar result was obtained for 2-MIB, as portrayed Figures 3 and 4. Therefore, the adsorption competition effect of NOM is expected to differ between S-PAC and PAC, and the adsorption competition effect is less severe on S-PAC than on PAC. The size reduction of carbon particle could be advantageous for removing both the NOM and the geosmin and 2-MIB by avoiding the adsorption competition effect.

Geosmin and 2-MIB adsorption in Hakucho and Suwannee humic acid waters

The initial TOC of Suwannee humic acid water (TOC, 1.6 mg/L) was higher than that of Hakucho water (TOC, 1.4 mg/L) in the adsorption experiments. It was therefore expected that the adsorption competition was more severe in Suwannee humic acid water than in Hakucho water. However, results show that the amounts of geosmin adsorbed onto S-PAC and PAC in the Hakucho water were about half of those in the Suwannee humic acid water, as presented in Figure 5. Therefore, NOM existing in the Hakucho water tends more to compete in adsorption with geosmin than NOM existing in the Suwannee humic water. One reason related to this different adsorption competition effect is the difference of the molecular weight distributions of NOMs in the Hakucho water and Suwannee humic acid water. The molecular weight of NOM contained in Hakucho water was lower than that of the Suwannee humic acid water, as depicted in Figure 6. Accordingly, Hakucho water probably has a greater tendency to compete in adsorption with low molecular weight compound of geosmin than Suwannee humic acid water. Moreover, Figure 4 presents that TOC adsorption capacity in the Hakucho water was greater than in the Suwannee humic acid water. These results indicate that natural water whose NOM adsorbs more on S-PAC and PAC might decrease the geosmin adsorption capacity more.

Comparison between the geosmin adsorption capacity and 2-MIB adsorption capacities

As shown in Figure 2, the geosmin adsorption capacity was decreased by one-fifth through adsorption competition by NOM of Hakucho water. However, according to Figure 3, the 2-MIB adsorption capacity was decreased more. It was decreased by one-tenth by the NOM. These results demonstrate that 2-MIB has a greater tendency to receive adsorption competition from NOM than geosmin. Geosmin has slightly lower MW than 2-MIB (geosmin 220 and

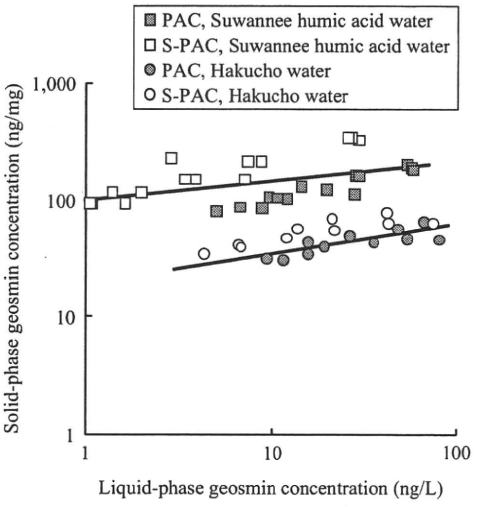

Figure 5 | Adsorption isotherms of geosmin in Hakucho water and Suwannee humic acid water (the lines are Freundlich model fits).

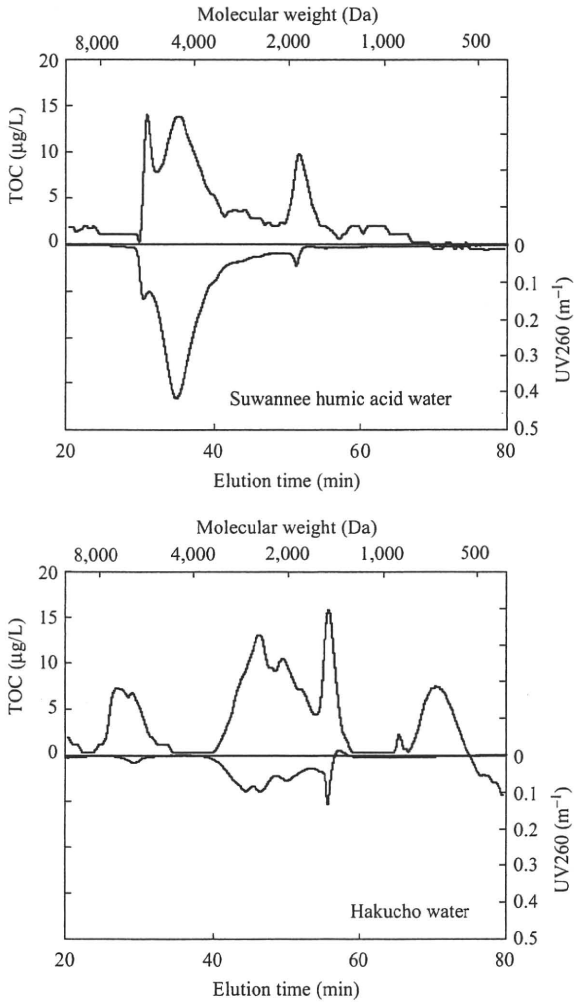

Figure 6 | Molecular weight distributions of NOMs in natural water.

2-MIB 206 Da), which might cause geosmin to have less severe adsorption competition from NOM, which has large MW, because adsorbates of similar MW would have high competition. Overall, the NOM competition effect observed for 2-MIB and geosmin on S-PAC and PAC is not straightforward and remains to be resolved.

CONCLUSIONS

(1) Geosmin adsorption capacities on S-PAC and PAC were not very different: the capacity on S-PAC was slightly higher than on PAC. Carbon particle size reduction did not largely change the geosmin adsorption.

(2) Although S-PAC adsorbed NOM more than PAC, the adsorption capacity of geosmin in natural water did not largely differ between S-PAC and PAC. Increased NOM adsorption through carbon particle size reduction did not influence the geosmin adsorption capacity.

(3) Adsorption competition with geosmin was severer in natural water including NOM of the lower molecular weight.

(4) Findings described in conclusions (1)–(3) for geosmin were also obtained for 2-MIB.

(5) 2-MIB shows a greater tendency to have adsorption competition with NOM than geosmin does.

ACKNOWLEDGEMENTS

This study was supported by Grant-in-Aid for Scientific Research A(21246083) from the Ministry of Education, Culture, Sports, Science and Technology of the Government of Japan, by a research grant from the Ministry of Health, Labour and Welfare, and by Metawater Co., Tokyo, Japan.

REFERENCES

Huang, C., Van Benschoten, J. E. & Jensen, J. N. 1996 Adsorption kinetics of MIB and geosmin. *J. Am. Water Works Assoc.* **88**(4), 116–128.

Matsui, Y., Fukuda, Y., Murase, R., Aoki, N., Mima, S., Inoue, T. & Matsushita, T. 2004 Micro-ground powdered activated carbon for effective removal of natural organic matter during water treatment. *Water Sci. Technol. Water Supply* **4**(4), 155–163.

Matsui, Y., Aizawa, T., Kanda, F., Nigorikawa, N., Mima, S. & Kawase, Y. 2007 Adsorptive removal of geosmin by ceramic membrane filtration with super-powdered activated carbon. *J. Water Supply Res. Technol.–Aqua* **56**(6–7), 411–418.

Matsui, Y., Ando, N., Sasaki, H., Matsushita, T. & Ohno, K. 2009 Branched pore kinetic model analysis of geosmin adsorption on super-powdered activated carbon. *Water Res.* **43**(12), 3095–3103.

Najm, I. N., Snoeyink, V. L., Suidan, M. T., Lee, C. H. & Richard, Y. 1990 Effect of particle size and background natural organics on the adsorption efficiency of PAC. *J. Am. Water Works Assoc.* **82**(1), 65–72.

Newcombe, G. & Cook, D. 2002 Influences on the removal of tastes and odours by PAC. *J. Water Supply Res. Technol.–Aqua* **51**(8), 463–474.

Waer, M. A. 2006 Taste and odor multiple barriers for a smelly situtation. *Opflow* **32**(6), 1–5.

WATER RESEARCH 44 (2010) 4127–4136

Available at www.sciencedirect.com

ScienceDirect

journal homepage: www.elsevier.com/locate/watres

Comparison of natural organic matter adsorption capacities of super-powdered activated carbon and powdered activated Carbon

Naoya Ando, Yoshihiko Matsui, Ryuji Kurotobi, Yu Nakano, Taku Matsushita, Koichi Ohno*

Graduate School of Engineering, Hokkaido University, N13W8, Sapporo 060-8628 Japan

ARTICLE INFO

Article history:
Received 10 November 2009
Received in revised form
21 May 2010
Accepted 24 May 2010
Available online 4 June 2010

Keywords:
NOM
Pore size
Humic
Fulvic
Isotherm

ABSTRACT

We examined the natural organic matter (NOM) adsorption characteristics of super-powdered activated carbon (S-PAC) produced by pulverizing commercially available, normal PAC to a submicron particle size range. The adsorption capacities of S-PAC for NOM and polystyrene sulfonates (PSS) with molecular weights (MWs) of 1.1, 1.8, and 4.6 kDa, which we used as model compounds, were considerably higher than those of PAC. The adsorption capacity increases were observed for all five types of carbon tested (two wood-based, two coconut-based, and one coal-based carbon). The adsorption capacities of S-PAC and PAC for polyethylene glycols (PEGs) with MWs of 0.3 and 1.0 were the same. The adsorption capacities of S-PAC for PEGs with MWs of 3.0 and 8.0 kDa were slightly higher than the adsorption capacities of PAC, but the difference in adsorption capacity was not as large as that observed for NOM and the PSSs, even though the MW ranges of the adsorbates were similar. We concluded that the adsorption capacity differences between S-PAC and PAC observed for NOM and PSSs were due to the difference in particle size between the two carbons, rather than to differences in internal pore size or structure, to differences in activation, or to non-attainment of equilibrium that resulted from the change in particle size. The difference in adsorption capacity between S-PAC and PAC was larger for NOM with a high specific UV absorbance (SUVA) value than for low-SUVA NOM. The larger adsorption capacities of S-PAC compared with PAC were explained by the larger specific external surface area per unit mass. We hypothesize that a larger fraction of the internal pore volume is accessible with carbon of smaller particle size because the NOM and PSS molecules preferentially adsorb near the outer surface of the particle and therefore do not completely penetrate the adsorbent particle.

1. Introduction

In water treatment plants, the addition of powdered activated carbon (PAC) prior to a solid–liquid separation process, such as sedimentation, deep filtration, or membrane filtration, is a simple and widely applied method for removing dissolved contaminants that cannot be removed by the separation process itself. Although the adsorption capacity of PAC is high, that capacity is not fully utilized if the PAC–water contact times are insufficient, because adsorbate uptake is slow. PAC

* *Corresponding author.* Tel./fax: +81 11 706 7280.
E-mail address: matsui@eng.hokudai.ac.jp (Y. Matsui).
0043-1354/$ – see front matter © 2010 Elsevier Ltd. All rights reserved.
doi:10.1016/j.watres.2010.05.029